

Performance studies on Cu_2SnS_3 films grown by sulfurization of evaporated Sn-Cu stack precursors

H. JIA, H. ZHANG, S. CHENG*, J. YU, Y. LAI

College of Physics and Information Engineering, and Institute of Micro-Nano Devices and Solar Cells, Fuzhou University, Fuzhou, 350108, P. R. China

Jiangsu Collaborative Innovation Center of Photovoltaic Science and Engineering, Changzhou, 213164, P. R. China

Cu_2SnS_3 (CTS) thin films were grown by sulfurization of vacuum thermal evaporated Sn-Cu metallic precursors in a $\text{H}_2\text{S}:\text{N}_2$ atmosphere. Different Cu/Sn composition ratios of the films were prepared to study the effect of Cu/Sn atomic ratio on the properties of the CTS thin films. The microstructures and Cu/Sn composition ratios of the films were characterized with X-ray diffraction and energy dispersive X-ray spectroscopy (EDS), respectively. The X-ray diffractograms show that the deposited films are exclusively oriented along the (111) direction. The optical absorption coefficient and band gap of the films were estimated by transmission and reflection spectra measured at room temperature. Highly crystallized *p*-type CTS thin films were achieved when the Cu/Sn ratio was about 2.0. They had high absorption coefficient of $\sim 10^4 \text{ cm}^{-1}$, suitable carrier concentration $\sim 10^{17} \text{ cm}^{-3}$, high mobility $\sim 10^0 \text{ cm}^2 \text{ v}^{-1} \text{ s}^{-1}$ and narrow optical band gap $\sim 0.9 \text{ eV}$. Therefore, CTS thin films are suitable as absorber materials of thin film solar cells.

(Received May 21, 2015; accepted September 29, 2016)

Keywords: Thermal evaporated, Cu_2SnS_3 thin film, Two-stage process, Cu/Sn ratio, Solar cell material, Absorber layer, *p*-type semiconductor

1. Introduction

In recent years, $\text{Cu}_2\text{ZnSnS}_4$ (CZTS) thin films have attracted widespread attention as absorber layers for solar cells. At present, CZTS thin film solar cells with efficiency more than 12% [1] has been obtained. However, the CZTS thin film is difficult to be formed because the quaternary compound is only stable in a small region of chemical potential [2]. Ternary compound Cu_2SnS_3 (CTS) thin film shows *p*-type conductivity and has a high optical absorption coefficient ($>10^4 \text{ cm}^{-1}$) [3-5] with a direct band gap of $\sim 1.3 \text{ eV}$ (tetragonal structure) or $\sim 0.9 \text{ eV}$ (cubic structure) [6]. The estimated theoretical light conversion efficiency is above 33% [7]. In addition, the constituent elements are non-toxic and abundant in nature. So it is also considered a promising candidate for thin film solar cell absorber materials, and compared to CZTS, it is easier to be formed. Therefore, there are lots of reports on CTS thin films by several research groups using different approaches, including sputtering [2, 4], evaporation [8, 9], successive ionic layer adsorption and reaction (SILAR)[10], electrodeposition [11], solid reactions [5, 12, 13], spray pyrolysis [14], and solvothermal synthesis [15]. However, the highest conversion efficiency of the CTS solar cell reported so far is 2.92% [8]. One possible reason

for this low efficiency is the poor crystallization and unfavorable morphologies of the CTS films. For ideal absorber layers of solar cells, columnar grains through the thickness of the films are desirable, and they can avoid grain boundaries along the horizontal direction that usually act as recombination centers for minority carriers [16]. Therefore, a high degree of crystallization is very important for the CTS thin films. In this paper, we investigate the influence of Cu/Sn ratio on the films in order to obtain the CTS films with good properties.

2. Experiments

CTS thin films were deposited on soda lime glass (SLG) substrates by vapor-phase sulfurization of thermal evaporated precursors. Source materials were 99.99% purity Sn powder and 99.99% purity Cu. The chamber pressure was about $\sim 10^{-6}$ Torr. The substrate temperature was maintained at 150°C . The deposition rate and thickness of the films were monitored using a FTM-V quartz oscillator placed just below the substrate holder. Sn thin films were firstly deposited on the glass substrates. The deposition rate and thickness of the films were kept at 2 \AA/s and 150 nm , respectively. Then Cu layers with

thicknesses of 90nm, 110nm, 130nm, 150nm, 170nm and 190nm were respectively deposited on the Sn films to get the Sn/Cu stack precursors with different Cu/Sn ratios. Finally, the samples were sulfurized in an electric furnace in the atmosphere of N₂+H₂S(8%) vapor at 460°C for 120 min.

The thickness of the films was measured by a TENCOR D100 stylus profiler. The morphologies and Cu/Sn composition ratios were studied by a scanning electron microscopy with an EDAX attachment (XL30 ESEM-TMP). The structure analysis were performed with a Philips X'Pert-MPD X-ray diffraction (XRD) system equipped with a Cu K α source ($\lambda=1.54060\text{\AA}$) and a Raman spectroscopy (RENISHAW with 532 nm). Optical measurements were done using a Cary 5000-Scan

UV-VIS-NIR Spectrometer equipped with an integrating sphere. Electrical properties were determined by a HMS 3000 Hall measurement system based on Van der Pauw method.

3. Results and discussion

The samples information is shown in Table 1. The Cu/Sn ratio of the CTS thin films is increased for Cu-poor precursors compared with the Cu/Sn ratio of precursor (sample C1-C4). On the other hand, the Cu/Sn ratio is hardly changed for Cu-rich precursors (sample C5-C6). This is considered to be due to sublimation of Sn₂S₃ from the sulfurized films [11].

Table 1. Composition ratios and thickness of the precursors and sulfurized films on SLG substrates.

Sample	Cu/Sn ratio		S/ Cu+Sn	Thickness (nm)	
	Precursor	Sulfurized		Precursor	Sulfurized
C1	1.41	1.64	1.13	243	471
C2	1.61	1.79	1.12	265	506
C3	1.77	1.97	1.10	284	552
C4	1.95	2.06	1.02	306	615
C5	2.14	2.17	1.01	323	651
C6	2.39	2.42	1.02	345	695

The X-ray diffractograms of the CTS films with different Cu/Sn ratios are shown in Fig. 1 The diffractograms show sharp peaks at 2θ values of 28.4°, 32.9°, 47.3° and 56.1° which match with those from cubic CTS (JCPDS089–2877) and are found to be reflections from (111), (200), (220) and (311) planes. These results accord with those reported by Fernandes, et al. [6]. It indicates that the films are polycrystalline CTS with a strong preferred orientation. With increasing Cu/Sn ratio, the intensity of diffraction peaks becomes relatively more intense and sharper for the Cu-poor samples (samples C1-C4). It indicates that the crystallinity of the CTS thin films is improved with increasing Cu/Sn ratio. However, it has the opposite trend for the Cu-rich samples (samples C5-C6). It is perhaps that some Cu₂SnS₃ changes into Cu₃SnS₄ under the condition of Cu-rich (Cu₂SnS₃ and Cu₃SnS₄ have the similar diffraction peaks). The same results can be obtained by analyzing the electrical properties of the samples. Baranowski, et.al. have obtained the same results[17]. In addition, peaks at 26.2°, and 31.2° are observed in the Sn-rich samples (C1-C4). These peaks

are attributable to orthorhombic Sn₂S₃ (JCPDS030–1377) phase. The presence of residual impurity phase in the thin films is considered to have a detrimental effect on the performance of the solar cells. The crystallite size of the samples can be estimated according to the Scherrer's equation as follows:

$$D = \frac{k\lambda}{\beta \cos(\theta)} \quad (1)$$

where k is a constant (0.89), λ the X-ray wavelength, β the full width at half maximum and θ the Bragg diffraction angle. Thus, the crystallite size of the sample calculated using the broadening of (111) line is about 30 nm, which remains the same for all the samples of different Cu/Sn ratios.

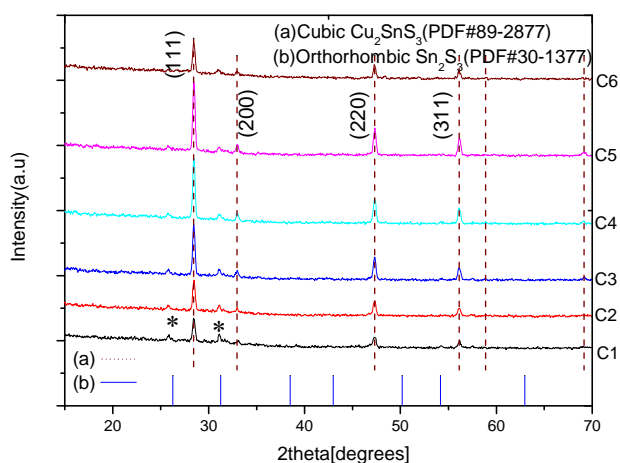


Fig. 1. XRD patterns of the CTS thin films at different Cu/Sn ratios.

For simplification, Fig. 2 only shows the Raman spectrum of sample C3. There are two main peaks located at 300 and 351 cm^{-1} which can be assigned to cubic Cu_2SnS_3 [18]. In addition, obvious peaks at 310 cm^{-1} can be clearly observed which is in good agreement with the reported Raman spectra of Sn_2S_3 [19]. Other samples have similar results.

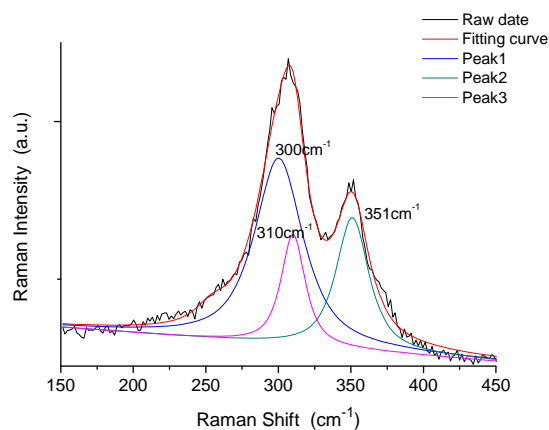


Fig. 2. Raman spectrum (532 nm excitation) of sample C3.

Fig. 3 shows the SEM images of samples C1–C6. In samples C1–C3, the images depict formation of large aggregates with porous coral like structures and the size of the grains is not uniform. Although similar morphology is also formed in samples C4–C6, the grains size is obviously uniform. The different film morphologies among the samples are probably due to the different amount losses of Sn element.

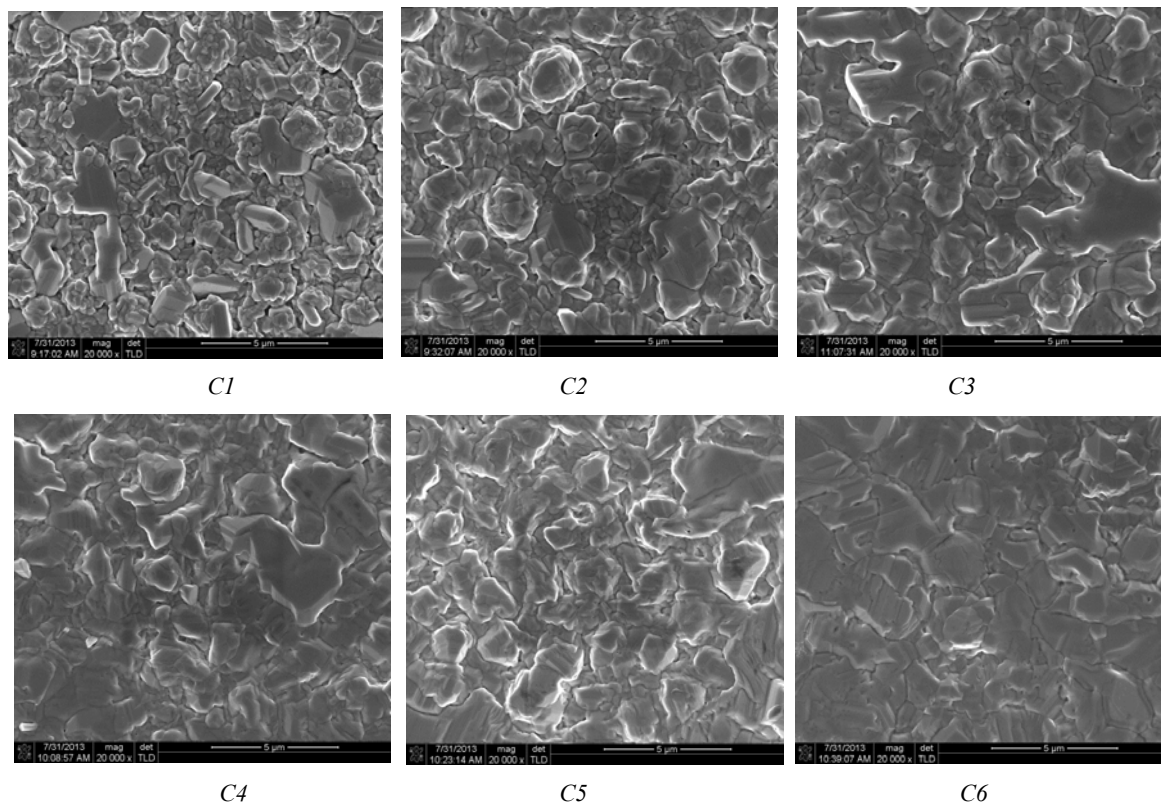


Fig. 3. SEM images of the CTS thin films at different Cu/Sn ratios.

To estimate the absorption coefficient (α) and the band gap of the fabricated CTS thin films, optical transmission and reflection spectra were measured in the wavelength 400-1600nm. The absorption coefficient can be calculated from the measured reflectance, transmittance and thickness of the films. Then we found a linear dependence indicating an allowed direct transition with:

$$\alpha hv = A(hv - E_g)^{1/2} \quad (2)$$

where E_g is the band gap, and A is a constant. The band gap is estimated by extrapolating the linear region of $(\alpha hv)^2$ vs hv to zero. Fig.4 only shows absorbance spectrum of sample C4 for simplification with the curve of $(\alpha hv)^2$ vs hv in the inset. The E_g and α near the fundamental edge of the CTS thin films are listed in Table 2. The E_g is slightly reduced from 0.98 eV of sample C1 to 0.88eV of sample C6 with increasing Cu/Sn ratio. Meanwhile, the absorption coefficient near the fundamental edge for all the samples is larger than $5.0 \times 10^4 \text{ cm}^{-1}$. These values are in good agreement with those reported in Ref. [3, 4].

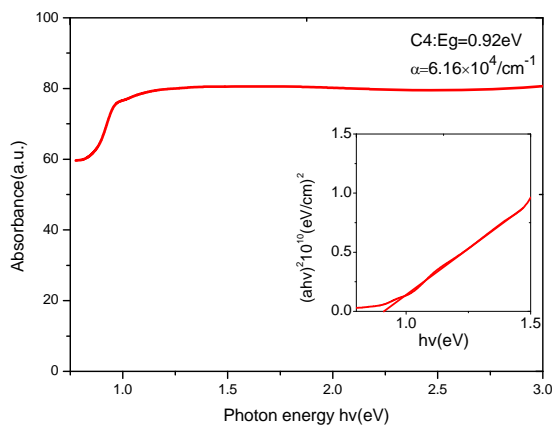


Fig. 4. Absorbance spectrum of sample C4. $(\alpha hv)^2$ vs hv curve is shown in the inset.

Table 2. Photoelectric characteristics of the CTS thin films with different Cu/Sn ratios.

Sample	$N_b/10^{17} \text{ cm}^{-3}$	$\mu / \text{cm}^2 \text{ v}^{-1} \text{ s}^{-1}$	$\rho/\Omega \cdot \text{cm}$	E_g/eV	$\alpha / 10^4 \text{ cm}^{-1}$
C1	3.72	1.752	9.574	0.98	7.74
C2	3.94	2.151	7.363	0.90	7.00
C3	2.29	3.447	7.912	0.91	6.51
C4	3.96	5.475	2.879	0.92	6.16
C5	7330	0.625	0.014	0.89	5.79
C6	8970	0.354	0.019	0.88	5.69

At room temperature, the semiconducting properties of the films were measured by the Hall measurement system. The results are listed in Table 2. All the samples are of p -type conductivity. The carrier concentrations of sample C5 and C6 are two orders of larger than those of samples C1-C4. Maybe some Cu_2SnS_3 changes into Cu_3SnS_4 under the condition of Cu-rich. It is in accordance with the analysis of Ref [17]. The carrier concentration and the mobility of samples C1-C4 are about $\sim 10^{17} \text{ cm}^{-3}$ and $\sim 10^0 \text{ cm}^2 \text{ v}^{-1} \text{ s}^{-1}$, respectively. These values are in good agreement with those reported in Ref. [3, 12].

4. Conclusion

The CTS thin films were deposited on the glass substrates by sulfurization of vacuum thermal evaporated Sn-Cu metallic precursors in a $\text{H}_2\text{S}:\text{N}_2$ atmosphere, and the effect of Cu/Sn ratios on the films were investigated. We find that highly crystallized single-phase CTS thin films are formed when the Cu/Sn ratio is about 2.0. The CTS films with a Cu/Sn ratio of ~ 2.0 shows a direct band gap of $\sim 0.9 \text{ eV}$, high optical absorption coefficient $> 10^4 \text{ cm}^{-1}$, suitable carrier concentration $\sim 10^{17} \text{ cm}^{-3}$ and mobility $\sim 10^0 \text{ cm}^2 \text{ v}^{-1} \text{ s}^{-1}$, which is suitable for PV application.

Acknowledgments

This work was supported by the National Nature Science Foundation of China (No. 61574038), Fujian Provincial Department of Science & Technology, China (2015H0021) and Fujian Provincial Department of Education (JA15091).

References

- [1] W. Wang, M. T. Winkler, O. Gunawan, et al. *Advanced Energy Materials* **4**(7), 2014.
- [2] H. T. Zhang, M. Xie, S. Zhang, et al. *Journal of Alloys and Compounds* **602**, 199 (2014).
- [3] D. Avellaneda, M. T. S. Nair, P. K. Nair, *Journal of The Electrochemical Society* **157**(6), D346 (2010).
- [4] P. A. Fernandes, P. M. P. Salomé, A.F. da Cunha, *Physica Status Solidi (c)* **7**(3-4), 901 (2010).
- [5] M. Bouaziz, J. Ouerfelli, S. K. Srivastava, et al. *Vacuum* **85**(8), 783 (2011).
- [6] P. A. Fernandes, P. M. P. Salome, A. F. da Cunha, *Journal of Physics D-Applied Physics* **43**(21), 215403 (2010).
- [7] D. Tiwari, T. K. Chaudhuri, T. Shripathi, et al. *Solid State Physics* **1447**, 1039 (2012).
- [8] N. Aihara, H. Araki, A. Takeuchi, et al. *Physica Status Solidi (c)* **10**(7-8), 1086 (2013).

- [9] K. Chino, J. Koike, S. Eguchi, H. Araki, R. Nakamura, K. Jimbo, H. Katagiri, *Japanese Journal of Applied Physics* **51**(10), 10NC35 (2012).
- [10] Z. Su, K. Sun, Z. Han, et al. *Journal of Materials Chemistry* **22**(32), 16346 (2012).
- [11] J. Koike, K. Chino, N. Aihara, et al. *Japanese Journal of Applied Physics* **51**(10), 10NC34 (2012).
- [12] D. Tiwari, T. K. Chaudhuri, T. Shripathi, et al. *Journal of Physics and Chemistry of Solids* **75**(3), 410 (2014).
- [13] X.-a Chen., H. Wada, A. Sato, et al. *Journal of Solid State Chemistry* **139**(1), 144 (1998).
- [14] M. Bouaziz, M. Amlouk, S. Belgacem, *Thin Solid Films* **517**(7), 2527 (2009).
- [15] Y. Tan, Z. Q. Lin, W. H. Ren, et al. *Materials Letters* **89**, 240 (2012).
- [16] T. Toyama, T. Konishi, Y. Seo, et al. *Applied Physics Express* **6**(7), 075503 (2013).
- [17] L. L. Baranowski, P. Zawadzki, S. Christensen, et al. *Chemistry of Materials* **26**, 4951 (2014).
- [18] P. A. Fernandes, P. M. P. Salomé, A.F. da Cunha, *Physica status solidi (c)* **7**(3-4), 901 (2010).
- [19] L. A. Burton, D. Colombara, R. D. Abellon, et al. *Synthesis, Chemistry of Materials* **25**(24), 4908 (2013).

*Corresponding author: sycheng@fzu.edu.cn
jasonhongjie@qq.com